



The domain of existence of prograde Rayleigh-wave particle motion for simple models

Peter G. Malischewsky^{a,*}, Frank Scherbaum^b, Cinna Lomnitz^c,
Tran Thanh Tuan^a, Frank Wuttke^d, Gadi Shamir^e

^a *Institut für Geowissenschaften, Friedrich-Schiller-Universität Jena, Burgweg 11, D-07749 Jena, Germany*

^b *Institut für Geowissenschaften, Universität Potsdam, Postfach 60 15 53, D-14415 Potsdam, Germany*

^c *Instituto de Geofísica, UNAM, 04510 Mexico, D. F., Mexico*

^d *Bauhaus-Universität Weimar, Bodenmechanik, D-99421 Weimar, Germany*

^e *Geophysical Survey of Israel (GSI), Jerusalem 95501, Israel*

Received 18 June 2007; received in revised form 28 September 2007; accepted 27 November 2007

Abstract

The existence of prograde particle motion for fundamental-mode Rayleigh waves is studied systematically in models of increasing complexity by using an exact expression of the ellipticity. This expression, together with the secular equation for the phase velocity, are useful to find the most relevant parameters for prograde particle motion, namely Poisson's ratio in the layer and the shear-wave velocity contrast between the layer and the half-space. The density contrast between layer and half-space, and up to a certain degree Poisson's ratio in the half-space, are usually less important. The domain of existence of prograde Rayleigh-particle motion is specified for typical combinations of parameters.

© 2008 Elsevier B.V. All rights reserved.

Keywords: Rayleigh waves; Ellipticity; Prograde motion

1. Introduction

It is well established in textbooks that Rayleigh waves propagating over the surface of a homogeneous elastic half-space feature retrograde particle motion (see e.g. Achenbach [1] and Kaufman and Levshin [2]). However, in the inhomogeneous half-space retrograde or prograde motion is possible depending on the frequency range. Early papers devoted to this subject include Giese [3] and Kisslinger [4]. Both found evidence of prograde Rayleigh motion in soils. Giese found prograde and retrograde wave groups in a model consisting of a layer on a rigid half-space. He calculated Poisson's ratio in the layer from the critical frequency where particle motion changes from prograde to retrograde. Mooney and Bolt [5] presented an extensive numerical study

* Corresponding author. Tel.: +49 3641948663; fax: +49 3641948662.

E-mail addresses: p.mali@uni-jena.de (P.G. Malischewsky), fs@geo.uni-potsdam.de (F. Scherbaum), cinna@prodigy.net.mx (C. Lomnitz).

about dispersion of the first three Rayleigh modes for a single surface layer. They also mentioned the change of particle motion under certain circumstances. Stephenson [6] discussed the restrictions on the emergence of prograde Rayleigh-wave particle motion in a soft-soil layer. Tanimoto and Rivera [7] provide the eigenfunctions of Rayleigh waves and their ratios numerically for a layer over a half-space. They found that Rayleigh-wave particle motion can become prograde near the surface when the structure contains a low-velocity sedimentary layer. Prograde Rayleigh-wave motion in a layered half-space was theoretically obtained by Wuttke [8]. Prograde Rayleigh waves were observed in the valley of Mexico by Gomez-Bernal [9], Lomnitz and Meas [10], and Stephenson et al. [11]. A theoretical derivation was provided by Malischewsky et al. [12].

For certain configurations of material parameters a pure modal analysis may become difficult or impossible for the practical process of extracting and identifying modes from real wave records (see e.g. Levshin and Panza [13]). This statement does not exclude the principal theoretical possibility. It happens especially when energy is transmitted through internal waveguides. In these cases, the dispersion curve, extracted from experimental data, is composed by parts of several different modes with the consequence that the concept of an individual mode loses its sense for practical purposes. The problem is closely related to the osculation of dispersion curves (see e.g. Sezawa and Kanai [14] and Forbriger [15]). On the other hand, the study of general properties of individual modes is of fundamental interest, as it is not always easy to know in advance when the modal theory will fail to apply.

This paper is organized as follows. We discuss the sense of particle motion in structural models of increasing complexity beginning with the homogeneous half-space, and continuing with an impedance surface, a layer with fixed bottom, and a layer over a half-space. The latter model involves some considerable complexities, and we have to confine our treatment to several special cases.

2. The homogeneous half-space

This case does not offer major difficulties and provides an opportunity of introducing some nomenclature, definitions and formulas for convenience. In most cases the terminology is the same of Malischewsky and Scherbaum [16]. Differences in notation will be noted. Consider plane harmonic Rayleigh waves with angular frequency ω , wave number k , and phase velocity $c = \omega/k$. The isotropic medium is characterized by Lamé parameters μ , λ and density ρ , whence we may obtain the velocities of longitudinal waves α and of transverse or shear waves β . The squared ratio of these velocities, which is a function of Poisson's ratio ν , is denoted by γ :

$$\gamma = \left(\frac{\beta}{\alpha}\right)^2 = \frac{1-2\nu}{2(1-\nu)}. \quad (1)$$

Let P , Q , p , q be defined as follows:

$$P = k^2 - k_\alpha^2, \quad Q = k^2 - k_\beta^2, \quad p = \sqrt{P}, \quad q = \sqrt{Q}, \quad (2)$$

where k_α and k_β are the wave numbers of longitudinal and transversal waves. A Cartesian coordinate system is assumed, where the x_1 axis points into the direction of propagation while the x_3 axis is directed into the half-space. The horizontal and vertical displacement components of Rayleigh waves $U_1(x_3)$ and $U_3(x_3)$ are the eigenfunctions, defined in the general manner as in Eq. (7) of Malischewsky and Scherbaum [16]. The horizontal component is real and the vertical component is purely imaginary. These definitions follow from the equations of motion and are valid in layers with finite thickness. In order to be valid for the half-space problem as well they must be specified in a straightforward manner as presented in [16]. It is well-known that the ellipticity χ for the stress-free surface ($x_3 = 0$) is then

$$\chi = i \frac{U_1(0)}{U_3(0)} = \frac{2\sqrt{1-c^2/\beta^2}}{2-c^2/\beta^2}, \quad (3)$$

where i is the imaginary unit. By using the simplified representation of the Rayleigh-wave velocity as a function of Poisson's ratio ν by Malischewsky [17] we obtain the ellipticity χ as a function of ν in the form:

$$\chi = \chi(v) = \frac{\sqrt{1 - 2g_4(v)}}{1 - g_4(v)} \quad (4)$$

with the abbreviations

$$g_3(v) = 17 + 3\sqrt{33 - 24\bar{v}^3 + \frac{321}{4}\bar{v}^2 - 93\bar{v} - \frac{45}{2}\bar{v}},$$

$$g_4(v) = \frac{1}{3} \left[4 + \frac{2(1 - 3\bar{v})}{\sqrt[3]{g_3(v)}} - \sqrt[3]{g_3(v)} \right] \quad \text{and} \quad (5)$$

$$\bar{v} = 1 - \frac{v}{1 - v}, \quad (6)$$

where the main values of the cubic roots should be used.

This ellipticity $\chi(v)$ is a positive function for $-1 \leq v \leq 0.5$ as a result of retrograde particle motion (see Malischewsky et al. [12]). The change of sign of χ in more complex structural models is precisely the cause of the change of sense of particle motion, as will be discussed below.

3. The impedance surface

The impedance surface is a low-frequency approximation to the “layer over a half-space” model after Tiersten (see Malischewsky and Scherbaum [16]). In this approach, the approximate equations of low frequency extension and flexure of thin plates are used in order to describe the influence of a thin layer over a half-space by replacing the stress-free condition on the surface by an impedance-like boundary condition on top of the half-space. An expression for the ellipticity χ was presented by Malischewsky and Scherbaum [16, Eq. (19)]. Fig. 3 in Ref. [16] contains an error which is corrected here. Consider a non-dimensional frequency \bar{f} , defined as

$$\bar{f} = d/\lambda_{\beta_1}, \quad (7)$$

where d is the thickness of the layer and λ_{β_1} is the wavelength of shear waves in the layer. We recompute χ for the impedance surface as a function of \bar{f} with the parameters of Model 1 (see Table 1). The result is presented in Fig. 1.

The ellipticity in the homogeneous half-space with stress-free boundary conditions is included as a dashed line for comparison. Notice that the dependence of χ on \bar{f} is weak, with a maximum at approximately $\bar{f} = 1$. It can be shown that χ has no singularity of the type that is common for many parameter combinations of a layer over half-space model (see Fig. 5 in [16]), and that χ does not vanish. Thus the particle motion does not change sense. It becomes clear from (3) that χ is always positive for zero frequency, i. e. the particle motion is retrograde for all models and frequencies.

4. Layer with fixed bottom

We are using the same eigenfunctions as in Eq. (7) of Malischewsky and Scherbaum [16], with a stress-free surface at $x_3 = 0$ and a fixed bottom at $x_3 = d$:

$$U_1(d) = U_3(d) = 0. \quad (8)$$

Table 1
Model parameters for the models under consideration

	Model 1	Model 2	Model 3
$r_s = \beta_1/\beta_2$	0.1667	0.2473	0.2473
$r_d = \rho_1/\rho_2$	0.7407	0.7391	0.7391
v_1	0.4375	0.5	0.4576
v_2	0.2506	0.5	0.3449

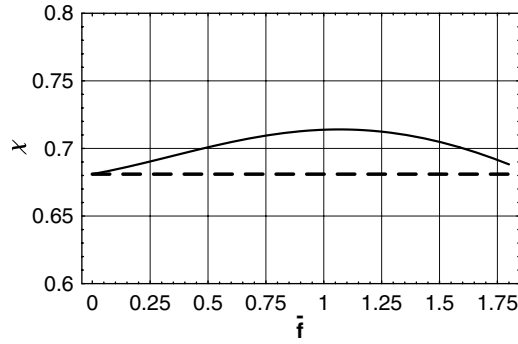


Fig. 1. The ellipticity for Rayleigh waves on an impedance surface (solid) and on a homogeneous half-space (dashed) in dependence on frequency.

Omitting some algebra we find for these boundary conditions the following secular determinant of the boundary-value problem:

$$\Delta_f = A_0 + B_0 \sinh\left(\frac{2\pi\bar{f}g_z}{C}\right) \sinh\left(\frac{2\pi\bar{f}g_\beta}{C}\right) + C_0 \cosh\left(\frac{2\pi\bar{f}g_z}{C}\right) \cosh\left(\frac{2\pi\bar{f}g_\beta}{C}\right) \quad (9)$$

where the abbreviations are

$$C = c/\beta, \quad g_z = p/k = \sqrt{1 - \gamma C^2}, \quad g_\beta = q/k = \sqrt{1 - C^2} \quad (10)$$

and the constants A_0 , B_0 , C_0 are given by

$$\begin{aligned} A_0 &= -4\gamma(C^2 - 2)g_z g_\beta, \\ B_0 &= \gamma[8 - 4C^2(2 + \gamma) + C^4(1 + 4\gamma)], \\ C_0 &= -\gamma g_z g_\beta(8 - 4C^2 + C^4). \end{aligned} \quad (11)$$

C is obtained by letting Δ_f vanish. From (1) and (9)–(11) we find for this model that the non-dimensional “phase velocity” C is a function of \bar{f} and v but not of the density:

$$C = C(\bar{f}, v). \quad (12)$$

The corresponding ellipticity χ_f may be determined as in Malischewsky and Scherbaum [16]. It is given by

$$\chi_f = \sqrt{1 - C^2} \cdot \frac{(2 - C^2) \cosh\left(\frac{2\pi g_z \bar{f}}{C}\right) - 2 \cosh\left(\frac{2\pi g_\beta \bar{f}}{C}\right)}{2g_z g_\beta \sinh\left(\frac{2\pi g_z \bar{f}}{C}\right) + (C^2 - 2) \sinh\left(\frac{2\pi g_\beta \bar{f}}{C}\right)} \quad (13)$$

which yields

$$\chi_f = \chi_f(\bar{f}, v). \quad (14)$$

A 2D graph of χ_f as a function of \bar{f} and v (Fig. 2) displays the sharp partition into two regions, where $\chi_f > 0$ corresponds to retrograde particle motion (dark shading) and $\chi_f < 0$ to prograde particle motion (light shading).

The domain of prograde motion is bounded on the left by a critical point P_1 with coordinates (0.25, 0.2026) and at the top of the figure by point P_3 with coordinates (0.5126, 0.5). Unfortunately, there is no algebraic representation of these coordinates. They follow from the solution of the system of Eq. (17) when $\gamma = 0$. A further critical point P_2 with coordinates ($\sqrt{3}/4$, 0.25) is located near the center of the graph. A more detailed explanation is beyond the treatment in this paper, as it requires a careful analytical treatment of the eigenvalue problem. However, let us summarize some main results of such an analysis without proof.

The critical value $v = 0.2026$ follows from the equation

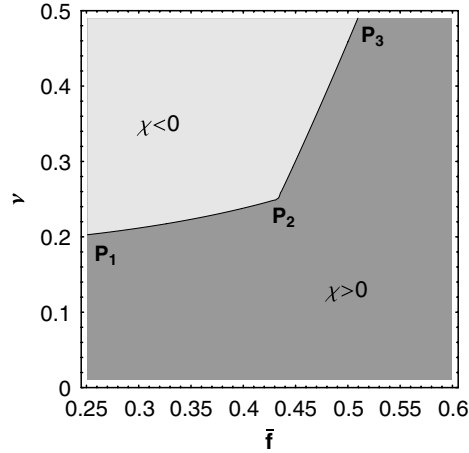


Fig. 2. The ellipticity for the model with fixed bottom in dependence on frequency and Poisson's ratio: retrograde motion (dark gray) and prograde motion (light gray).

$$1 - 2\sqrt{\gamma} \sin\left(\frac{\pi}{2}\sqrt{\gamma}\right) = 0. \quad (15)$$

No prograde motion is observed for $\nu < 0.2026$. The same critical value is observed in the method used by Giese [3] for the determination of Poisson's ratio from frequency when the sense of motion changes. The curves and P_1P_2 and P_2P_3 in Fig. 2 are obtained from the numerical solutions of

$$\begin{aligned} \bar{f} &= \frac{C}{2\pi g_\alpha} \operatorname{arcosh}\left(\sqrt{\frac{\gamma(1-C^2) + C^2/4}{\gamma(1-C^2) + 1}}\right), \\ \bar{f} &= \frac{C}{2\pi g_\beta} \operatorname{arcosh}\left(\frac{2}{2-C^2} \sqrt{\frac{\gamma(1-C^2) + C^2/4}{\gamma(1-C^2) + 1}}\right), \end{aligned} \quad (16)$$

and

$$\begin{aligned} \bar{f} &= \frac{C}{2\pi g_\beta} \operatorname{arcosh}\left(\sqrt{\frac{\gamma(1-C^2) + C^2/4}{\gamma(1-C^2) + 1}}\right), \\ \bar{f} &= \frac{C}{2\pi g_\alpha} \operatorname{arsinh}\left(\frac{2}{2-C^2} \sqrt{\frac{\gamma(1-C^2) + C^2/4}{\gamma(1-C^2) + 1}}\right), \end{aligned} \quad (17)$$

where arsinh and arcosh are the respective inverse hyperbolic functions.

The critical point P_2 is closely connected with a so-called osculation point of dispersion curves for the fundamental and first higher modes, respectively. At this point, $\bar{f} = \sqrt{3}/4$, $C = 2$, $\nu = 0.25$, and χ_f becomes indeterminate as

$$\chi_f = \frac{0}{0} \text{ for } \bar{f} = \sqrt{3}/4 \text{ and } \nu = 0.25 \quad (18)$$

with right-hand and left-hand limits

$$\lim_{\bar{f} \rightarrow \sqrt{3}/4+0} \chi_f = 0.4089 \quad \text{and} \quad \lim_{\bar{f} \rightarrow \sqrt{3}/4-0} \chi_f = -7.3371. \quad (19)$$

This remarkable jump had been noticed, among others, by Giese [3]. It is an example of the problems with mode theory, as encountered under certain circumstances mentioned in the introduction. A discussion and explanation of this behaviour is definitely beyond the scope of this article. The crucial point to avoid such dif-

faculties (like this jump) is to classify the eigenfunctions or modes in another manner as pointed out already by Okal [18] in the context of the Earth's spheroidal modes. We have only considered the fundamental mode which is defined in the standard manner as the wave with the lowest phase velocity. If instead the branches are defined by continuity of dc/df , allowing them to cross each other, then the discontinuity disappears (both “new” branches present continuous phase and group velocity and ellipticity at P_2). Similar points appear for higher modes at higher frequencies. From mathematical point of view that is a degeneration of eigenvalues, which we observe for the fundamental mode, however, for $v = 0.25$ only.

We note that for frequencies below $\bar{f} = 0.25$ there is no undamped surface-wave motion. This is a special feature of the model with fixed bottom. Further, for high frequencies there can be only retrograde motion because of the skin effect in surface waves: high-frequency waves are concentrated within a thin layer near the surface. For negative Poisson ratios (auxetic materials), which are not included in Fig. 2, we observe always retrograde motion.

5. A layer over a half-space

Let us denote the parameters of the layer with index 1 and of half-space with index 2. We omit the explicit derivation of the secular determinant Δ_I as it can be found in different forms in textbooks (e.g., Ben-Menahem and Singh [19]). We consider the arguments of this determinant:

$$\Delta_I = \Delta_I(r_s, r_d, v_1, v_2, C, \bar{f}), \quad (20)$$

where we introduce the ratios

$$r_s = \beta_1/\beta_2, \quad r_d = \rho_1/\rho_2, \quad (21)$$

and C defined for this model as c/β_1 and \bar{f} as d/λ_{β_1} .

Now the vanishing of Δ_I yields C . Note that for constant r_s , C as a function of \bar{f} does not depend on β_1 . It is well-known that the influence on C of r_s and v_1 is much greater than that of r_d and v_2 . Malischewsky and Scherbaum [16] presented an explicit expression for the H/V ratio of a layer over a half-space. This is a convenient starting-point for the investigation of the sense of particle motion. For convenience we reproduce this formula by adopting the following definitions (Malischewsky and Scherbaum [16]):

$$\begin{aligned} p_1 &= \sqrt{k^2 - k_{\alpha_1}^2}, \quad p_2 = \sqrt{k^2 - k_{\alpha_2}^2}, \quad q_1 = \sqrt{k^2 - k_{\beta_1}^2}, \quad q_2 = \sqrt{k^2 - k_{\beta_2}^2}, \\ g_1 &= p_2 q_1 k^2 (m_2 m_4 + 2f_1 m_1 m_3), \\ g_2 &= -2k^2 p_1 q_1 (m_1 m_2 - 2m_3 p_2 q_2 \delta\mu), \\ g_3 &= k^2 (m_2 m_5 - 2f_1 p_2 q_2 m_3^2), \\ g_4 &= 2k^2 p_1 q_1 (m_1 m_2 - 2m_3 p_2 q_2 \delta\mu), \\ g_5 &= -2p_1 q_1 k^2 (f_1 m_1^2 + p_2 q_2 m_4 \delta\mu), \\ g_6 &= 2k^2 p_1 q_2 (f_1 m_1 m_3 - m_5 \delta\mu), \end{aligned} \quad (22)$$

where

$$\begin{aligned} \delta\mu &= \rho_1 \beta_1^2 - \rho_2 \beta_2^2, \quad \delta\rho = \rho_1 - \rho_2 \quad \text{and} \\ m_1 &= 2k^2 \delta\mu + \omega^2 \rho_2, \\ m_2 &= 2k^2 \delta\mu - \omega^2 \delta\rho, \\ m_3 &= 2k^2 \delta\mu - \omega^2 \rho_1, \\ m_4 &= -4k^2 \delta\mu + 2\omega^2 (\rho_1 - \rho_2 \beta_2^2 / \beta_1^2), \\ m_5 &= 4k^4 \delta\mu + \omega^4 \delta\rho / \beta_1^2 + 2k^2 \omega^2 [\rho_2 (\beta_2^2 / \beta_1^2 + 1) - 2\rho_1]. \end{aligned} \quad (23)$$

A quantity y is defined as follows:

$$y = \frac{g_1 \cosh(dq_1) + g_2 \sinh(dp_1) + g_3 \sinh(dq_1)}{g_4 \cosh(dp_1) + g_5 \cosh(dq_1) + g_6 \sinh(dq_1)}, \quad (24)$$

and the ratio $\chi = H/V$ may be written as

$$\chi = \left(1 - \frac{c^2}{2\beta_1^2}\right) \times \frac{1}{\sqrt{1 - c^2/\alpha_1^2}} \times \frac{1 + y \tanh(dp_1)}{y + \tanh(dp_1)}. \quad (25)$$

It can be shown that χ is a function of the following arguments:

$$\chi = \chi(r_s, r_d, v_1, v_2, \bar{f}). \quad (26)$$

We note that β_1 does not enter separately into this analytical representation of the ellipticity with the consequence that the absolute value of the shear-wave velocity in the layer does not influence the sense of the particle motion. The domain of existence of prograde motion for this model is very involved to investigate in a general way. We must be satisfied with investigating the role of the two leading parameters r_s and v_1 . It can be demonstrated numerically that the influence of r_d and v_2 on the ellipticity is less relevant in many cases. On the other hand, we have also been able to ascertain an interesting influence of v_2 on the value of the ellipticity in certain cases.

For simplicity, we begin with an incompressible structural model (see Model 2 in Table 1). We show the influence of r_s and \bar{f} on the domain of prograde motion in Fig. 3. The region of prograde Rayleigh motion ($\chi < 0$) is shown in red. The fine structure of positive H/V -values in the domain of retrograde motion is also shown in shades of blue, with the lighter shades corresponding to the higher values.

Because of the skin effect of surface waves and recalling that the Rayleigh motion is retrograde in the homogeneous half-space, prograde motion should be expected only in a certain range of frequencies \bar{f} . From Fig. 3 this is indeed the case. For very low r_s (i. e. for a high shear-wave contrast), we observe prograde motion approximately in the interval $0.25 \leq \bar{f} \leq 0.5$, which falls between the so-called fundamental frequency of the site $\beta_1/4d$ and the double site frequency $\beta_1/2d$. Malischewsky et al. [12] point out that the vertical and horizontal eigenfunctions change signs at these frequencies: this is responsible for the occurrence of prograde motion. The fundamental site frequency is important in seismic hazard assessment as it is connected with the shear-wave resonance in the layer.

The exact upper limit of \bar{f} for prograde motion is 0.5126 which corresponds to the critical point P_3 from Section 4. The ratio of shear-wave velocities r_s was caused to vary between 0.01 and 0.9. For $r_s > 0.2$ the frequency range of prograde motion becomes narrower and finally it vanishes for r_s greater than about 0.5. As pointed out by Malischewsky et al. [12], the behaviour of the function χ can be tricky; thus prograde motion can be challenging to calculate numerically in certain ranges. The domain of prograde motion may be

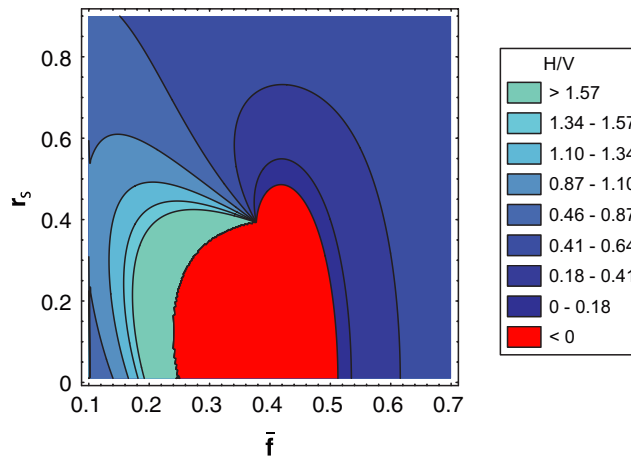


Fig. 3. 2D graph of the domain of prograde motion (red) as a function of \bar{f} and r_s for the incompressible Model 2. Retrograde motion in shades of blue depending on the values of χ . The value $r_s = 0$ corresponds to the fixed-bottom model (FBM).

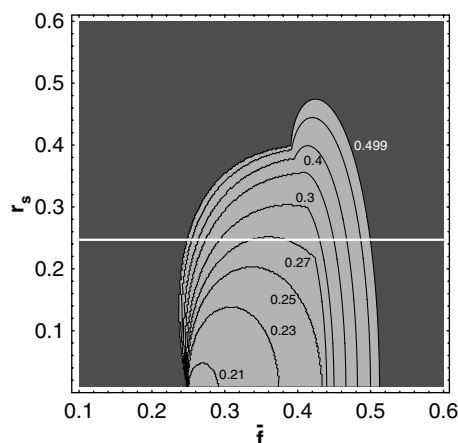


Fig. 4. 2D graph of the range of prograde motion (light grey) as a function of \bar{f} and r_s for different values of ν_1 (contours) and for r_d and ν_2 of Model 3. The white horizontal line corresponds to $r_s = 0.2473$ in Model 3 and $r_s = 0$ corresponds to FBM.

bounded either by two zeros in χ , by two poles, or more commonly by a pole and a zero. In Fig. 3, there is a remarkable point on the boundary of the red region, at $\bar{f} \approx 0.377$ and $r_s \approx 0.393$. It can be shown that for $r_s < 0.393$ the prograde domain is bounded on the left by a pole, but for $r_s > 0.393$ it is bounded by a zero.

Model 3 from Table 1 may be regarded as an example of the influence of the layer's Poisson ratio ν_1 on the sense of particle motion. In Fig. 4, the parameters were chosen to include the simplified configuration of the Kiryat Shmona test site in the Dead Sea transform fault region, Israel [20], which is of interest in seismic hazard analysis. The parameters of the test site are $\beta_1 = 0.45$ km/s, $\beta_2 = 1.82$ km/s, $\rho_1 = 1.7$ g/cm³, $\rho_2 = 2.3$ g/cm³, $d = 0.042$ km.

Fig. 4 is organized as in Fig. 3. The domain of prograde motion is light grey and that of retrograde motion is dark grey. The domain of prograde motion is bounded by the contour $\chi = 0$ for $\nu_1 = 0.499$. Thus the domain of prograde motion is maximal for an incompressible layer. Contours of $\chi = 0$ for $\nu_1 = 0.21, 0.25, 0.27, 0.3, 0.4, 0.458$ are included to show that the domain of prograde motion becomes smaller for low Poisson ratios and disappears for $\nu_1 < 0.2026$. This value matches the critical point P_1 from Section 4. The contour for $\nu_1 = 0.458$ is relevant for the Kyriat Shmona test site. It is located between 0.4 and 0.499. The corresponding shear-wave ratio $r_s = 0.2473$ for this model is indicated by the horizontal white line. Thus the domain of prograde motion is practically within the maximal frequency range $0.25 \leq \bar{f} \leq 0.5126$.

Note the peculiar shape of the contours between 0.27 and 0.3. The steep slopes at $r_s \approx 0.22$ for $\nu_1 \approx 0.27$ and $r_s \approx 0.3$ for $\nu_1 \approx 0.3$ are related with osculation of dispersion curves, a phenomenon which occurs at these “edge-points”. A more careful numerical analysis shows that for fixed ν_2 and r_d these steep contours occur for $0.25 \leq \nu_1 \leq \nu_c$, where ν_c is a critical Poisson's ratio. For our parameter set ν_c is about 0.34.

The steep contours have a remarkable property. The domain of prograde motion is limited by two poles in χ when r_s is situated between the edge and the top of the corresponding contour. Only for these situations two poles of χ can occur. Thus there is a close connection between the H/V - theory and osculation.

Figs. 3 and 4 were calculated by using the ContourPlot command of MATHEMATICA® version 4.0.

6. Conclusions

We have shown that Tiersten's impedance surface cannot support prograde Rayleigh motion. However, prograde motion is observed for a layer with fixed bottom and a layer over a half-space within some domains of frequency, Poisson's ratio, and shear-wave contrast. For a layer with a fixed bottom, prograde particle motion is present in the frequency range of $0.25 \leq \bar{f} \leq 0.5126$ if Poisson's ratio is greater than about 0.2026. It is concluded that Giese's method is applicable only for Poisson's ratios above 0.2026. The general validity of a lower limit $\nu_1 = 0.2026$ of Poisson's ratio and of an upper frequency limit $\bar{f} = 0.5126$ for prograde Rayleigh motion should not be underestimated. These limits are valid for all models of the layer over half-space type, not only for a layer with fixed bottom.

The prograde particle motion domain for a layer over a half-space depends strongly on Poisson's ratio ν_1 in the layer and on the shear-wave contrast r_s . However, the absolute value of the shear-wave velocity in the layer is not relevant for the existence or non-existence of prograde Rayleigh particle motion. The influence of the density contrast r_d and in many cases also of Poisson's ratio ν_2 in the half-space is less relevant; however especially the latter influence should be examined in detail in future. We have been able to demonstrate the influence of the osculation of dispersion curves on the behaviour of the ellipticity: this too should be studied more thoroughly.

We have discussed some fundamental properties of Rayleigh waves. The prograde or retrograde character of Rayleigh particle motion should yield useful additional constraints on uniqueness of the inversion of dispersion and ellipticity measurements of Rayleigh waves. These considerations should turn out to have a considerable impact on the characterization of site response in seismic hazard assessment.

Acknowledgements

P.G.M. thanks Prof. A. L. Levshin of the University of Colorado, Boulder, USA, and Dr. Th. Forbriger of the University Karlsruhe, Germany for useful discussions. The authors are thankful to Dr. V. Pinsky of GII, Lod, Israel for a reference and model parameters for the Kiryat Shmona test site. This work was supported by the Deutsche Forschungsgemeinschaft (DFG) under Grant No. MA 1520/6-2. Further, P.G.M. and G.S. gratefully acknowledge the support of Bundesministerium für Bildung und Forschung (BMBF) in the framework of the joint project "WTZ Germany-Israel: System Earth" under Grant No. 03F0448A.

References

- [1] J.D. Achenbach, Wave Propagation in Elastic Solids, Elsevier, New York, 1984.
- [2] A. Kaufman, A.L. Levshin, Acoustic and Elastic Wave Fields in Geophysics III, Elsevier, Amsterdam, 2005.
- [3] P. Giese, Determination of elastic properties and thickness of friable soils by using special Rayleigh waves (in German), Gerl. Beitr. Geophysik 66 (1957) 274–312.
- [4] C. Kisslinger, Observations of the development of Rayleigh-type waves in the vicinity of small explosions, J. Geophys. Res. 64 (1959) 429–436.
- [5] H.M. Mooney, B.A. Bolt, Dispersive characteristics of the first three Rayleigh modes for a single surface layer, Bull. Seism. Soc. Am. 56 (1966) 43–67.
- [6] W.R. Stephenson, Factors bounding prograde Rayleigh-wave particle motion in a soft-soil layer, in: Proceedings of the 2003 Pacific Conference on Earthquake Engineering, 13–15 February 2003, Christchurch, New Zealand, New Zealand Society of Earthquake Engineering.
- [7] T. Tanimoto, L. Rivera, Prograde Rayleigh wave motion, Geophys. J. Int. 162 (2005) 399–405.
- [8] F. Wuttke, Contribution to site identification using surface waves (in German), Ph.D. thesis, Bauhaus University Weimar, 2005.
- [9] A. Gómez-Bernal, Interpretation of soil effect in the Mexico valley using high density arrays of accelerographs, Ph.D. thesis, UNAM, Mexico, 2002.
- [10] C. Lomnitz, Y. Meas, Huygens' principle. The capture of seismic energy by a soft soil layer, Geophys. Res. Lett. 31 (2004) L13613, 1029/2004GL019910.
- [11] W.R. Stephenson, C. Lomnitz, H. Flores, Late resonant response at Texcoco, Valley of Mexico, during distant earthquakes, Soil Dyn. Earthq. Eng. 26 (2006) 791–798.
- [12] P.G. Malischewsky Auning, C. Lomnitz, F. Wuttke, R. Saragoni, Prograde Rayleigh-wave motion in the valley of Mexico, Geofísica Internacional 45 (2006) 149–162.
- [13] A.L. Levshin, G.F. Panza, Caveats in multi-modal inversion of seismic surface wavefields, Pure Appl. Geophys. 163 (2006) 1215–1233.
- [14] K. Sezawa, K. Kanai, Discontinuity in the dispersion curves of Rayleigh waves, Bull. Earthq. Res. Inst. 13 (1935) 237–244.
- [15] T. Forbriger, Inversion of shallow seismic wavefields (in German), Ph.D. thesis, University Stuttgart, 2001, <http://elib.uni-stuttgart.de/opus/volltexte/2001/861>.
- [16] P.G. Malischewsky, F. Scherbaum, Love's formula and H/V -ratio (ellipticity) of Rayleigh waves, Wave Motion 40 (2004) 57–67.
- [17] P.G. Malischewsky Auning, A note on Rayleigh-wave velocities as a function of the material parameters, Geofísica Internacional 45 (2004) 507–509.
- [18] E.A. Okal, A physical classification of the Earth's spheroidal modes, J. Phys. Earth 26 (1978) 75–103.
- [19] A. Ben-Menahem, S.J. Singh, Seismic Waves and Sources, Springer-Verlag, New-York, 1981.
- [20] M. Ezersky, V. Shtivelman, Seismic refraction surveys for updating the microzonation map of Israel, Report No. 802/43/99, 1999, prepared for the Earth Sciences Research Administration, The Ministry of National Infrastructures.